

Infinite reduction in absorbing time in quantum walks over classical ones

Shuva Mondal^{1,*}, Amrita Mandal^{1,2†} and Ujjwal Sen^{1‡}

¹*Harish-Chandra Research Institute, A CI of Homi Bhabha National Institute, Chhatnag Road, Jhunsi, Prayagraj 211019, India and*
²*National Institute of Technology Agartala, Agartala 799046, India*

We study the absorption time and spreading rate of the discrete-time quantum walk propagating on a line in the presence or absence of an absorber. We analytically establish that in the presence of an absorber, the average absorption time of the quantum walker is finite, contrary to the behavior of a classical random walker, indicating an infinite resource reduction on moving over to a quantum version of a walker. Furthermore, numerical simulations indicate a reversal of this behavior due to the insertion of disorder in the walker's step lengths. Additionally, we demonstrate that in the presence of an absorber, there is a speed-up in the spreading rate, and that a disordered quantum walk that is sub-ballistic regains the ballistic spreading of a clean quantum walk.

I. INTRODUCTION

Over the past few decades, there have been several developments in the area of quantum information and computation, for example, quantum dense coding, quantum algorithms, etc. [1, 2], and quantum walk is one of them that provides a universal quantum computational framework [3, 4]. The coined quantum random walk (QRW) model comprises a walker and a coin that controls the movement of the walker [5–8]. QRWs differ from classical random walks (CRWs) through different features and characteristics such as superposition, interference, and reversible unitary time evolution [9–12]. As a result of these distinctive characteristics, quantum walks show ballistic spreading, where the walker's position expands with time or the number of steps [13, 14]. In contrast to this, the spreading rate of classical random walks is diffusive in nature and is proportional to the square root of time [15]. The consequences of the ballistic nature of QRWs show diverse applications in the areas including quantum search algorithms [16–19], triangle finding problem [20], evaluating NAND trees [21, 22], and a platform for studying topological phases [23–25] with applications involving ultra-cold rubidium atoms. In addition, the classical counterpart of QRW is a well-studied topic in various fields, such as the modeling of Brownian motion [26, 27], estimating the volume of a convex body using Markov chain models [28], modelling boson hopping [29, 30], and the PageRank algorithm [31, 32].

QRWs have been extensively studied for both discrete [33, 34] and continuous time steps [35, 36]. In this paper, we focus on the former one. In discrete-time quantum walks (DTQWs), at each time step, the walker moves through discrete lattice points [37–39]. The evolution of the walker of a DTQW can be hindered by the presence of different unavoidable environmental effects, such as disorder or noise [40, 41]. The term disorder in a quan-

tum system refers to the introduction of randomness or imperfections into the system, potentially having a substantial effect on the behavior and properties of the quantum particle. Quantum walks with disorder have been studied by considering disorders in the displacement operations [42–47] or in the coin operations [48–60]. The presence of disorder exhibits significant influence on the spreading behavior of the walker, that generally inhibits the ballistic spreading and results in partial or complete localization [61].

Disorder can be added into the system by introducing random variations in the potential landscape or the hopping amplitudes, or it may appear due to the unavoidable interaction between the system and the environment. In the context of QRWs, the disorder can be categorized into two distinct forms: static disorder and dynamic disorder [62–64]. Static disorder involves a position-dependent random variable that represents a fixed, random arrangement of impurities in a lattice, which remains constant over time. The randomized parameters in static disorder suppress quantum evolution, which can lead to phenomena like Anderson localization [65–67]. The dynamic disorder is characterized by a position- and time-dependent random variable, which involves fluctuations or vibrations in the lattice over time, resulting in decoherence. This induces a quantum-to-classical transition [51, 63, 64, 68, 69]. The presence of an absorber can have a substantial influence on the dynamics of the QRWs as well. If the quantum particle is detected at the absorber's site, it gets absorbed, thereby terminating the walk [70–72]. Absorber introduces a non-unitary effect into the evolution of quantum walk, which results into interesting phenomena like absorption probability and exists probability [73, 74].

The rest of this paper is organized as follows. Section II introduces the theoretical framework for quantum walks and the spreading rate of walks. In Section III the effect of an absorber in DTQW is described. There we also presented our 1st result about finite average absorbing time for DTQW in contrast to classical random walk in the presence of an absorber. There we also presented our numerical findings on how things get reversed if there is disorder in the lengths of steps of the walker. Sec-

* shuvamondal@hri.res.in

† mandalamrita55@gmail.com, amrita.math@faculty.nita.ac.in

‡ ujjwal@hri.res.in

tion IV presents how the presence of an absorber affects the spreading rate of a walker even when the steps of the walker are disordered. Finally, Section V concludes the paper and outlines future research directions.

II. DTQW ON A LINE

In this section, we briefly discuss the discrete-time quantum walks (DTQWs) on a line. In DTQW, the system is described by a state vector defined in the Hilbert space $\mathcal{H} = \mathcal{H}_p \otimes \mathcal{H}_c$, where the Hilbert spaces \mathcal{H}_c and \mathcal{H}_p denote the coin and the position spaces, respectively. The Hilbert space $\mathcal{H}_c = \text{span} \{ |L\rangle, |R\rangle \}$ describes the two-dimensional coin space where $\{ |L\rangle, |R\rangle \}$ forms the canonical ordered basis for \mathbb{C}^2 and, L and R stand for left and right directions of the walker. The infinite-dimensional position space \mathcal{H}_p is defined as $\mathcal{H}_p = \text{span} \{ |m\rangle \mid m \in \mathbb{Z} \}$, where $|m\rangle$ indicates the position vector of the walker on the 1D lattice \mathbb{Z} . Hence, the total Hilbert space is $\mathcal{H} = \text{span} \{ |m, l\rangle \mid m \in \mathbb{Z}, l \in \{L, R\} \}$. The DTQW propagates through the lattice by performing two operations on the walker's state at each time step, the coin tossing operation C followed by the shift operation S . Thus, the evolution operator for the walk takes the form

$$W = S(I \otimes C), \quad (1)$$

where I is the identity operator acting on \mathcal{H}_p . Hence, after t time steps, the state of the walker becomes $|\psi_t\rangle = W^t |\psi_0\rangle$, where $|\psi_0\rangle$ is the initial state of the walker.

The action of the coin operator $C = \begin{bmatrix} a & b \\ c & d \end{bmatrix}$ is described as, $C |L\rangle = a |L\rangle + b |R\rangle$, $C |R\rangle = c |L\rangle + d |R\rangle$, where $\{a, b, c, d\} \in \mathbb{C}$ are chosen accordingly depending on the choice of the coin operator. For example, in the case of the Hadamard walk, that is described by the single qubit Hadamard gate H as the coin operator,

$$a = -b = -c = -d = -\frac{1}{\sqrt{2}}. \quad (2)$$

The shift operator S is defined as

$$S = \sum_{n=-\infty}^{\infty} |n-1, L\rangle \langle n, L| + |n+1, R\rangle \langle n, R|, \quad (3)$$

and its action on the basis states is given by $S |n, L\rangle = |n-1, L\rangle$, $S |n, R\rangle = |n+1, L\rangle$. Finally, from Eq. (1) we get

$$\begin{aligned} W |n, L\rangle &= a |n-1, L\rangle + b |n+1, R\rangle \\ W |n, R\rangle &= c |n-1, L\rangle + d |n+1, R\rangle. \end{aligned} \quad (4)$$

Let the initial state of the walk be expanded as

$$|\psi_0\rangle = \sum_n \psi_0^L(n) |n, L\rangle + \psi_0^R(n) |n, R\rangle,$$

where $\psi_0^L(n)$ and $\psi_0^R(n)$ are the probability amplitudes of the coin states $|L\rangle$ and $|R\rangle$, respectively, at position

n and at time $t = 0$. Then, by applying W on $|\psi_0\rangle$ for t times, we get

$$\begin{aligned} |\psi_t\rangle &= W^t \left(\sum_n \psi_0^L(n) |n, L\rangle + \psi_0^R(n) |n, R\rangle \right) \\ &= \sum_n \psi_t^L(n) |n, L\rangle + \psi_t^R(n) |n, R\rangle. \end{aligned}$$

Hence, the probability of the walker to be at the position n after time t is given by

$$\begin{aligned} p(n, t) &= |\langle n, L | \psi_t \rangle|^2 + |\langle n, R | \psi_t \rangle|^2 \\ &= |\psi_t^L(n)|^2 + |\psi_t^R(n)|^2. \end{aligned}$$

The standard deviation σ , that quantifies the spreading rate of the walk, can be expressed in terms of the position probability distribution $p(n, t)$ as follows.

$$\sigma = \sum_n n^2 p(n, t) - \left(\sum_n n p(n, t) \right)^2.$$

Now the dependence of σ on time t can be scaled by the exponent α as

$$\sigma \propto t^\alpha. \quad (5)$$

From Eq. (5), it is evident that α describes how the nature of the walker spreading changes with time. For example [7], α takes value 1 in clean DTQWs.

III. INFINITE ABSORBING TIME IN CLASSICAL WALK VS FINITE DURATION IN THE QUANTUM CASE

In this section, we review the effects on the evolution of the clean CRW due to the presence of the absorber and analyze the same for clean DTQW. Physically, the walker stops its propagation while crossing the absorber that is present on the line of the walker's propagation, and the probability of moving to the subsequent position beyond the absorber gets absorbed. So, the walker can not move to the other side of the absorber. The probability to be at the other side of the absorber and the probability to be at the position of the absorber are lost.

Let p_t denotes the probability of being absorbed for the first time after t tosses at m_1 , the position of the absorber. Then, the total probability of absorption after considering all the time steps is

$$P = \sum_{t=1}^{\infty} p_t. \quad (6)$$

Let us denote t_a as the average absorbing time, and it is defined as

$$t_a = \frac{\sum_{t=1}^{\infty} t p_t}{\sum_{t=1}^{\infty} p_t}. \quad (7)$$

Note that the total probability of absorption P needs not be 1, and hence, we have to divide with P to define t_a in a meaningful way. In the following, we discuss the quantities (6) and (7) for both classical and quantum cases in detail.

A. Classical walk

In CRW, if the distance of the absorber from the starting position is $|m_1|$, then p_t is nonzero only if $t \geq m_1$, and $\frac{t+m_1}{2}$ is an integer. From [75], we get

$$p_t = \frac{|m_1|}{t \times 2^t} \frac{t!}{\left(\frac{t+m_1}{2}\right)! \left(\frac{t-m_1}{2}\right)!}.$$

Further, it can be shown that P as described in Eq. (6), is equal to 1 for CRW (see Appendix B). So that, for a classical random walk, the expression of the average time of absorption becomes

$$t_a = \sum_t t p_t = \sum_t \frac{|m_1|}{2^t} \frac{t!}{\left(\frac{t+m_1}{2}\right)! \left(\frac{t-m_1}{2}\right)!}, \quad (8)$$

where if m_1 is even (odd), the sum over t ($\geq m_1$) runs over the even (odd) numbers. We show that t_a is not finite for a clean CRW by proving the divergence of the infinite series sum (see Appendix C for the detail).

B. Quantum walk

In DTQW, the absorption probabilities (p_t) can be derived from amplitudes a_t of getting absorbed after time t by the relation $p_t = |a_t|^2$. Now these a_t can be calculated by defining the generating function $G(z)$ described as

$$G(z) = \sum_{t>0} a_t z^t, \quad (9)$$

where z is a complex variable. This $G(z)$ depends on the walker's initial state, the coin operator, and the position of the absorber. For example, consider DTQW with H as the coin operator, and the absorber is at the position m_1 . Then, if $|0, R\rangle$ is the initial vector, we get $G(z) = (g(z))^{m_1}$, otherwise, if $|0, L\rangle$ is the initial state, $G(z) = f(z)(g(z))^{m_1-1}$, [76] where

$$f(z) = \frac{1 + z^2 - \sqrt{1 + z^4}}{\sqrt{2}z},$$

$$g(z) = \frac{1 - z^2 - \sqrt{1 + z^4}}{\sqrt{2}z}.$$

Here, we have assumed $m_1 > 0$, but $m_1 < 0$, then $f(z)$ and $g(z)$ exchange their aforesaid expressions. From now onwards, unless not stated explicitly, we use H as coin, $|0, L\rangle$ as the initial state, and $m_1 = 2$ as the position of the absorber, so that when the walker gets absorbed its

state is described as $|2, R\rangle$. Under such circumstances, $G(z)$ in Eq. (9) simplifies to

$$G(z) = \frac{1 - \sqrt{1 + z^4}}{z^2}. \quad (10)$$

Now, expanding Eq. (10) in powers of z we get,

$$G(z) = \sum_{m=1}^{\infty} (-1)^m \frac{[2(m-1)]!}{2^{2m-1}(m-1)!m!} z^{4m-2}. \quad (11)$$

It is clear from the above power series that we get nonzero amplitude only when the corresponding toss number t equals to $4m-2$, and hence, we write the expression of the amplitudes by introducing the Kronecker delta function as

$$a_t = \sum_{m \in \mathbb{N}} (-1)^m \frac{[2(m-1)]!}{2^{2m-1}(m-1)!m!} \delta_{t,(4m-2)}.$$

So that the absorption probabilities become

$$p_t = \sum_{m \in \mathbb{N}} \left(\frac{[2(m-1)]!}{2^{2m-1}(m-1)!m!} \right)^2 \delta_{t,(4m-2)}. \quad (12)$$

Now, using (6) the total absorption probability P is written as

$$P = \sum_{m=1}^{\infty} \left(\frac{(2m-2)!}{2^{2m-1}(m-1)!m!} \right)^2.$$

The series sum in the right-hand side of the above expression of P converges and yields a total absorption probability value $P = \frac{4}{\pi} - 1$. From (7), the average absorbing time t_a becomes,

$$t_a = \frac{\sum_{m=1}^{\infty} (4m-2) \left(\frac{(2m-2)!}{2^{2m-1}(m-1)!m!} \right)^2}{\sum_{m=1}^{\infty} \left(\frac{(2m-2)!}{2^{2m-1}(m-1)!m!} \right)^2}. \quad (13)$$

The infinite series in the numerator of Eq. (13) converges (See Appendix C for details). Further, it can be derived that this series sum in the numerator takes the value $\frac{\pi-2}{\frac{\pi}{2}}$. So that the average absorption time can be approximated as $t_a = \frac{\pi-2}{\frac{\pi}{2}(\frac{4}{\pi}-1)} \approx 2.66$.

It is clear that as the position of the absorber shifts, the total absorbing probability P and the corresponding average absorbing time t_a change as well. We collect all these data in Table I, considering the absorber's position at the lattice points $1, \dots, 10$ on the line. It is evident from the table that the total absorbing probability gradually decreases and the average absorbing time increases as the distance between the starting point and the position of the absorber increases. In all such cases, we see that there is a linear relation between the average time of getting absorbed and the distance of the absorber from the starting position of the quantum walker. However, a reverse relation is observed for the total probability of getting absorbed with the absorber position.

m_1	P	t_a
1	0.64	1.57
2	0.27	2.66
3	0.18	4.87
4	0.16	7.48
5	0.15	10.07
6	0.14	12.91
7	0.14	15.50
8	0.14	18.07
9	0.14	20.61
10	0.14	23.39

TABLE I. Here m_1 , P and t_a denote the absorber's position, the total probability of absorption, and the average time of getting absorbed at m_1 , respectively. These values are approximated up to two decimal places. It is to be noted that t_a increases linearly with the distance of the absorber from the starting position of the quantum walker. Besides, an inverse relation is noticed between m_1 and P .

An interesting quantum mechanical impact on the average absorbing time of a walker in the presence of an absorber is that the classical walker cannot get absorbed after finite time steps; in contrast, the quantum walker does the same in finite time whenever the absorber is placed at a finite distance from the starting position of the walker. We notice that the absorption probabilities (p_t) carry the same values and hence lead to almost similar results while using the Kempe coin [7], instead of the Hadamard one.

C. Effects in the presence of disorders

In this section, we discuss the effects on the average absorbing time by introducing disorder in the walker's steps, both in classical and quantum scenarios. First, for a single realization of the disorder insertion, we calculate the weighted average time quantity

$$t_a^{(n)} = \frac{\sum_{t=1}^n t p_t}{\sum_{t=1}^n p_t}, \quad (14)$$

for a fixed n . Then, we consider Eq. (14) for different values of n , and for several such disorder realizations, we take the average of the quantity defined in Eq. (14) to get the disorder-averaged absorbing time $\langle t_a^{(n)} \rangle$ of the disordered walks. Here, the symbol $\langle \cdot \rangle$ stands for an average of the argument over the corresponding disorder realizations.

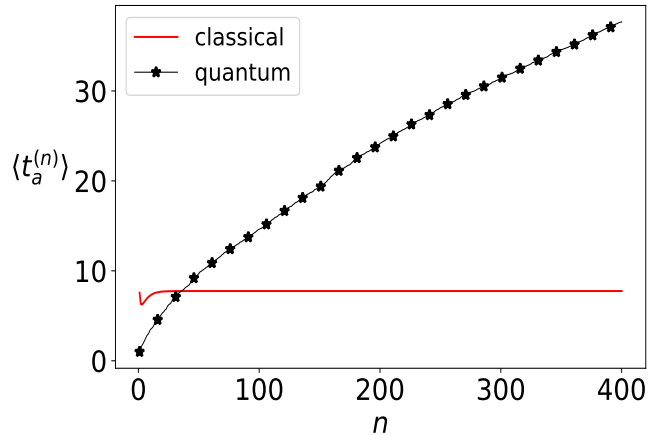


FIG. 1. A comparison of the disorder-averaged absorbing time of CRW and DTQW, both with the presence of an absorber at the position 2. The Poisson distribution with unit mean is the underlying disorder. The red line, without any marker, corresponds to the disordered-CRW. This plot shows a sudden fall at the beginning and no significant change is observed in the $\langle t_a^{(n)} \rangle$ values after few initial steps. As n increases, $\langle t_a^{(n)} \rangle$ attends a constant value of 7.75 (approximately), showing the convergence nature of $(\langle t_a^{(n)} \rangle)_n$ for the classical walk. Here, we have considered numerical simulations up to $n = 400$ steps. The black, asterisk-marked plot shows the behavior of the disorder-averaged absorbing time of disordered-DTQW defined by the Hadamard coin. This plot exhibits the monotonically increasing nature of $(\langle t_a^{(n)} \rangle)_n$, within the considered range of n values up to 400 steps ($\langle t_a^{(n)} \rangle \approx 38$ at $n = 400$). This signifies that $(\langle t_a^{(n)} \rangle)_n$ diverges for the DTQW we considered. Here, the averaged time quantity is derived over 40 different disorder realization runs.

We plot the n values along the horizontal axis and corresponding disorder-averaged time quantity $\langle t_a^{(n)} \rangle$ along the vertical axis for disordered-CRW and disordered-DTQW in Fig. 1. Here, we have considered discrete random outputs that follow the Poisson distribution with unit mean as the disorder insertion. The red line without any marking, representing disordered-CRW in Fig. 1, clearly illustrates that there is no significant change in the values of $\langle t_a^{(n)} \rangle$ after a certain finite steps. This indicates that for the classical walk, the sequence of disorder-averaged absorbing time $(\langle t_a^{(n)} \rangle)_n$ converges to a finite value with respect to n . On the other hand, the black asterisk marked line in Fig. 1 depicts an increase in n value resulting in a gradual increment of $\langle t_a^{(n)} \rangle$, when the disordered steps are chosen from the Poisson distribution with the specified parameters. This clearly shows the divergent nature of the sequence $(\langle t_a^{(n)} \rangle)_n$ with respect to the step size n , for the quantum case, when the disordered steps are collected from the Poisson distribution with unit mean.

We have also found similar behavior for $\langle t_a^{(n)} \rangle$ in disordered-DTQW, when the disordered step lengths are chosen from the other four types of discrete probability

distribution, i.e., binomial, negative binomial, geometric, and hypergeometric distributions with different parameter setup. In all such cases, $\langle t_a^{(n)} \rangle$ increases monotonically with n . This enlargement in $\langle t_a^{(n)} \rangle$ demonstrates the divergent nature of the disorder-averaged absorbing time, analogous to the Poisson disorder-averaged absorbing time in disordered-DTQW. Thus, considering all the discussions, we state that the behavior of the average time of absorption is altered in the presence of disorders for both classical and quantum walks.

IV. ABSORBER RENDERS DISORDER IRRELEVANT IN SPREADING RATE OF QUANTUM WALK

In this section, we study the impacts of an absorber on the spreading rate of DTQWs propagating in a 1D line. Additionally, we execute a comparative study of the spreading behavior of CRWs and DTQWs under such circumstances. In the present study, the spreading rate is quantified in terms of the exponent α as stated in Eq. (5). It is well known that in a clean CRW, where no absorber is present along the path of the walker, the probabilities show a diffusive normal distribution with standard deviation $\sigma \propto t^{\frac{1}{2}}$, and therefore $\alpha = 0.50$ [75]. At the same time, for a clean DTQW, where an absorber is not present, α is exactly equal to 1 and the walk is called ballistic in nature [17]. This quadratic speed up in the quantum regime exhibits the quantum advantages of random walks over the classical ones.

We observe that insertion of several disorders into the step lengths results in no significant change in the spreading of the 1D CRWs, and α almost remains 0.50. On the other hand, it has been demonstrated in [44] that for a disordered DTQW, the exponent α reduces noticeably and lies between $\frac{1}{2}$ and 1. Hence, the DTQW becomes sub-ballistic but super-diffusive in nature. In particular, for the Poissonian disorder (see Appendix A) insertion, if we take an average of several runs of the unit mean Poisson-distributed disorders, α drops to $\alpha \approx 0.70$ from $\alpha = 1$. So, even though the spreading of a CRW remains unaffected by step-length disorders, certain changes in the propagation of quantum walks are observed.

Now, we turn to the situation where an absorber is placed along the line of dispersion of the random walk. Then, the probability of existence of the particle should be drained. In order to obtain accurate findings, we need to adjust the remaining probability following the probability leakage due to the absorber. In the classical scenario, to make the modification, the probability at each position is divided by the total remaining probability, i.e., the total probability that the particle is not absorbed yet. The presence of the absorber does not have an impact on the spreading rate, and α remains 0.50. In the quantum regime, we renormalize the wave function over the locations where the absorption does not occur. In Fig. 2, we draw and compare the probability distributions of

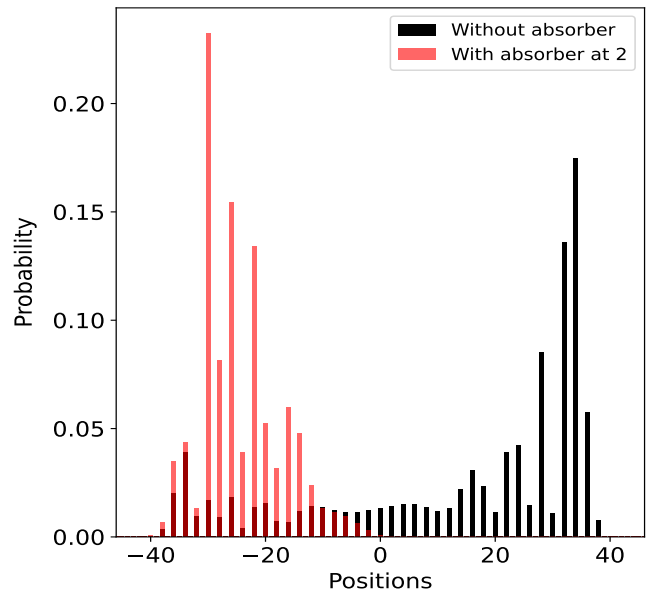


FIG. 2. Probability distribution of 1D-DTQW. This position-probability plot describes the probability distribution nature of the 1D-DTQW after 50 time steps, starts with the initial state $|0\rangle \otimes |0\rangle$. Here, the black vertical lines quantify the probability of the walker being at the specified positions on the line, when there is no absorber on the line. Here some higher probability values are observed along the positive nodes (right-hand side) compared to the other side. On the other hand, the red colour represents the case when there is an absorber at position 2. As a result of the absorber present at node 2, most of the non-zero probabilities are noticed along the negative nodes, with the highest peak around -32.

clean Hadamard 1D-DTQWs against some nodal positions, when the absorber is absent and present at a vertex of the line graph after some certain time-steps. In both cases, the walkers start from the position 0 with initial state $|0\rangle$, and snapshots for the probability distributions are taken after 20 times of evolution. Clearly, due to the presence of the absorber, a certain difference between the two position-probability distribution graphs is noticed, indicating different statistical characteristics of the distributions.

Furthermore, we observe that for 1D-DTQW with the (single-qubit) Hadamard coin, the scaling exponent α decreases slightly from 1 when an absorber is present. To determine this α , we first compute and collect standard deviations (σ) for some values of time t . Then, we create a graph of $\ln(\sigma)$ against $\ln(t)$ and fit it with a straight line with 95% confidence level. The slope of this line now signifies the exponent α , as defined in Eq. (5). Figure 3 shows the plot $\ln(\sigma)$ versus $\ln(t)$ of 1D Hadamard walk for $t \leq 80$, when the absorber is placed at the node 2 on the line. This results in an exponent value of 0.96 ± 0.005 with confidence level 95%, other than that of $\alpha = 1$, which occurs for quantum walks in the absence of the absorber. This decreased α value is also observed for placing the

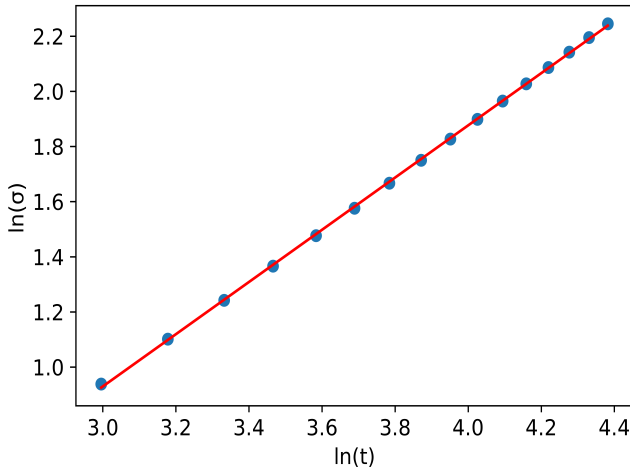


FIG. 3. Plot of $\ln(\sigma)$ against $\ln(t)$. The linear fitting (on the log-log plot) for the data points (blue colored dots) corresponding to the Hadamard 1D-DTQW with one absorber placed at 2 is represented by red solid line. With 95% confidence level, the slope of the fitted line falls within the confidence intervals 0.96 ± 0.005 , with an average least square error of 0.002 for the linear fittings. To ensure fewer errors in the fitting, we have chosen the t -range $20 < t < 80$.

absorber at other nodes as well, asserting the effectiveness of the absorber in the spread of the DTQWs.

Finally, we undertake the condition where CRWs or 1D-DTQWs are treated in the presence of glassy disorders in the walkers' step lengths, and absorbers at a node on the walker's line of propagation. Under these circumstances, we study the walk statistics and provide a comparative view with all the results discussed earlier. Fig. 4 represents a comparative view of the position-probability distributions after 20 time steps of disordered 1D-DTQW defined by the single qubit Hadamard coin, without and with the presence of an absorber on the line graph. In both cases, the walkers start from the position 0 and the initial coin state is $|0\rangle$. Now, to predict the spreading rate of the disordered walk, we consider the walk in different runs, as stated in Section III. In each run, the walk is treated by taking steps of random lengths drawn from a set of integers that follow a given probability distribution with some fixed parametric values. We call this process a single disorder realization of the walk. Then, for several such disorder realizations, we numerically evaluate σ , the measure of spreading of the walk. Then, we take the average of the σ s over all the disorder realizations to get $\langle\sigma\rangle$. Now, to find the spreading rate, we first plot $\ln(\langle\sigma\rangle)$ along the vertical against $\ln(t)$ along the horizontal and fit a straight line through the points with a minimum possible error of fitting, using the least squares method. The slope of the fitted straight line signifies the disorder-averaged spreading rate.

In the presence of an observer, the disordered CRWs for different probability distributions with different

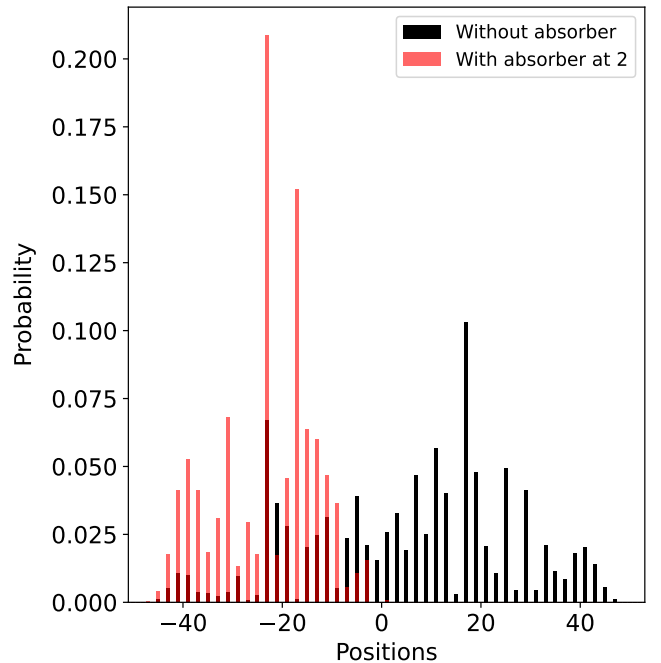


FIG. 4. Diagram of probability distribution of 1D Poisson disordered-DTQW defined by Hadamard coin after 50 evolutions, for a single disorder realization with mean value 1, without and with the presence of the absorber. In both cases, the walker starts from 0 node with initial coin state $|0\rangle$, and the outcomes of the Poisson distribution of unit mean in a single run are taken as the disorder realizations. The black color lines show probability distributions of disordered-DTQW over different locations, without the presence of any absorber. The red bars represent the position-probability distribution of disordered-DTQW, where an absorber is kept at node 2. In contrast to the no absorber case, non-zero probabilities are seen to be more localized near the starting position 0 when the absorber is placed.

strengths show no significant changes in spreading rate compared to the clean walk or the walk in the absence of an absorber. For Poisson disordered CRWs with mean 1, a pictorial view in support of the last line is provided in Fig. 5. It is worth observing that both lines have an equal slope (0.51), which signifies the diffusive nature of the corresponding walks as like a clean CRW with no absorber case. In contrast, when an absorber is added to a disordered DTQW regime, the spreading rate is enhanced, and the walk almost restores the ballistic nature of a clean DTQW. First, we start analyzing this phenomenon with the Poisson distributed disorders of unit mean. Fig. 6 depicts the change of $\ln(\langle\sigma\rangle)$ along the vertical direction against $\ln(t)$ along the horizontal. Here, to calculate $\langle\sigma\rangle$ we take the average over 1100 disorder realization sets. In this plot, we use a log-log (natural log) scale for better understanding of the relation. Using the method of least squares, we fit a straight line to the data set. The slope of the straight line is evaluated as 0.98 ± 0.004 , which is the value of the exponent α . Here,

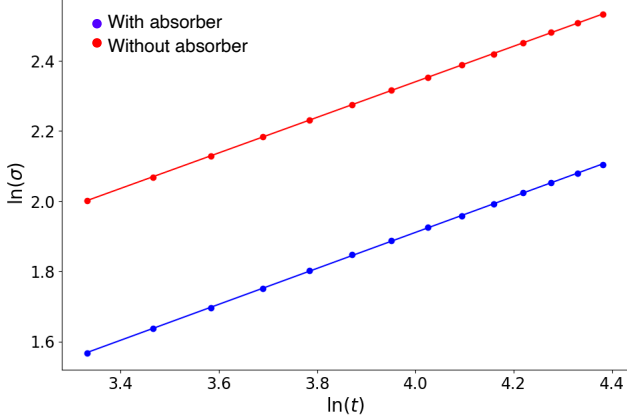


FIG. 5. (Color online.) $\ln(\sigma)$ against $\ln(t)$ for disordered (Poisson distribution) CRWs with and without absorber scenarios. Here, t ranges between 20 and 80. The red and blue fitted lines represent the cases without and with an absorber, respectively. Red line equation is $\ln(\sigma) = 0.51 \ln(t) + 0.31$, and the blue line is $\ln(\sigma) = 0.51 \ln(t) - 0.14$. The slopes of both lines are the same.

Distribution	Variance	Absorber present	α
Binomial	$\frac{1}{2}$	yes	1.02
		no	0.79
Hypergeometric	$\frac{4}{9}$	yes	1.03
		no	0.81
Negative Binomial	2	yes	0.91
		no	0.69
Geometric	2	yes	1.01
		no	0.74

TABLE II. Numerically evaluated values of the exponent α , corrected up to the second decimal places, for various discrete disorders with the distribution mean value 1, for all the cases. Corresponding variances for the distributions are listed in the second column. In all such instances, except with the negative binomial distribution, α increases to 1 approximately, after the insertion of an absorber on the walker's line of movement. For the negative binomial distribution, restoration of the α values towards the transition from sub-ballistic to ballistic, also shows a consistency with the other cases. Thus, the sub-ballistic spreading of disordered DTQWs, with random step lengths following sub- or super-Poissonian distributions, turns into a ballistic-like nature.

the numerical figures are corrected up to two significant figures; for more details on the process, we refer to [77]. We continue the process for other Poisson disorders with different strengths. This signifies that after the insertion of an absorber along the walker's line, a Poisson disordered DTQW, which was sub-ballistic and super-diffusive initially, regains the ballistic-like spreading as that of a clean DTQW.

In TABLE II, we provide a list of numerically evaluated exponent values of disordered DTQWs, for a variety

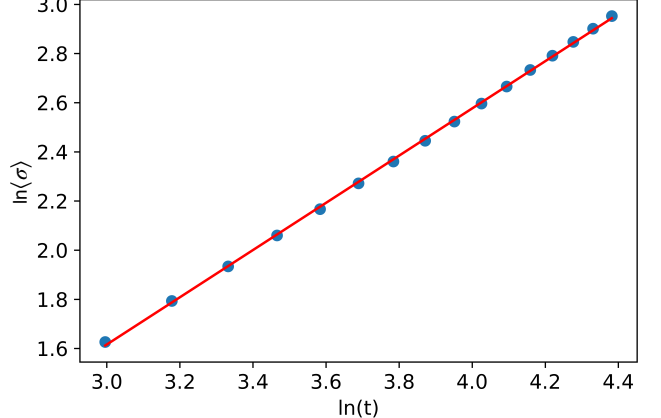


FIG. 6. (Color online.) Plot of $\ln(\langle \sigma \rangle)$ vs $\ln(t)$ for the disordered-DTQW with one absorber placed at the position 2 on the 1D line. The red solid line represents the linear fitting (on the log-log plot) for the data points (blue colored dots) corresponding to the Poisson disordered (mean 1) 1D-DTQW. The slope of the fitted line lies within the confidence intervals 0.98 ± 0.004 , with 95% confidence level, with an average least square error of 0.002 for the linear fittings. Here, t varies from 20 to 80.

of discrete probability distributions, all with unit mean value. We see that even if the distribution is different from the Poisson distribution, the presence of an absorber renders the effects of disorders irrelevant by restoring the rate of spreading of a disordered DTQW to that of a clean one.

V. CONCLUSION

In this article, we focus on how the presence of an absorber affects a one-dimensional discrete-time quantum walk. First, we define the average absorbing time and analytically show that this quantity diverges for a 1D classical random walk for any arbitrary choice of the absorber's position. Then, we prove that the average absorbing time for a 1D discrete-time quantum walk converges when the absorber is placed at the node 2. Also, for other positions of the absorber, we calculate the finite average absorbing time numerically. Moreover, if we induce disorders in the step lengths of the walks, this behavior of the walks is altered, i.e., the average absorbing time for CRW and DTQW converges and diverges, respectively. For a numerical establishment of the claim, we undertake the disordered step lengths that follow either of the Poisson, sub-Poisson, and super-Poisson discrete probability distributions.

Next, we discuss the influence of an absorber in the spreading and analyze the corresponding statistical properties of random walks. We observe that for the Poisson distributed disorders, the presence of an absorber enhances the spreading rate of the disordered quantum

walker, whereas it remains unchanged in the classical regime. Furthermore, we generalize this concept to sub- and super-Poissonian disorders as well, with different strengths. In fact, in all such instances, due to the presence of an absorber, the sub-ballistic nature of disordered DTQWs almost turns into a ballistic one. Thus, the absorber renders step-length disorders insignificant by restoring the spreading as a clean walk. Studying the effects of the absorber on average absorbing time, spreading rate, etc., of DTQWs for disorders in the coin operations, and whether the behavior persists as discussed in this paper, is a problem of future interest.

ACKNOWLEDGMENTS

We acknowledge discussions with Subhasis Jena. We thank the cluster facilities at the Harish-Chandra Research Institute. We acknowledge partial support from the Department of Science and Technology, Government of India through the QuEST grant (grant number DST/ICPS/QUEST/Theme-3/2019/120).

[1] V. M. Kendon, A random walk approach to quantum algorithms, *Philosophical Transactions of the Royal Society A: Mathematical, Physical and Engineering Sciences* **364**, 3407 (2006).

[2] A. Montanaro, Quantum algorithms: an overview, *npj Quantum Information* **2**, 1 (2016).

[3] A. M. Childs, Universal computation by quantum walk, *Phys. Rev. Lett.* **102**, 180501 (2009).

[4] A. M. Childs, D. Gosset, and Z. Webb, Universal computation by multiparticle quantum walk, *Science* **339**, 791–794 (2013).

[5] Y. Aharonov, L. Davidovich, and N. Zagury, Quantum random walks, *Phys. Rev. A* **48**, 1687 (1993).

[6] A. Nayak and A. Vishwanath, Quantum walk on the line, *arXiv preprint quant-ph/0010117* (2000).

[7] J. Kempe, Quantum random walks: an introductory overview, *Contemporary Physics* **44**, 307 (2003).

[8] A. Ambainis, Quantum walks and their algorithmic applications, *International Journal of Quantum Information* **1**, 507 (2003).

[9] J. R. Norris, *Markov chains*, 2 (Cambridge university press, 1998).

[10] F. Spitzer, *Principles of random walk*, Vol. 34 (Springer Science & Business Media, 2001).

[11] A. M. Childs, E. Farhi, and S. Gutmann, An example of the difference between quantum and classical random walks, *Quantum Information Processing* **1**, 35 (2002).

[12] J. Rudnick and G. Gaspari, *Elements of the random walk: an introduction for advanced students and researchers* (Cambridge University Press, 2004).

[13] N. Konno, Quantum random walks in one dimension, *Quantum Information Processing* **1**, 345 (2002).

[14] V. Kendon and B. Tregenna, Decoherence in discrete quantum walks, in *Decoherence and Entropy in Complex Systems: Selected Lectures from DICE 2002* (Springer, 2003) pp. 253–267.

[15] A. Ambainis, E. Bach, A. Nayak, A. Vishwanath, and J. Watrous, One-dimensional quantum walks, in *Proceedings of the Thirty-Third Annual ACM Symposium on Theory of Computing*, STOC '01 (Association for Computing Machinery, New York, NY, USA, 2001) p. 37–49.

[16] N. Shenvi, J. Kempe, and K. B. Whaley, Quantum random-walk search algorithm, *Physical Review A* **67**, 052307 (2003).

[17] R. Portugal, *Quantum walks and search algorithms*, Vol. 19 (Springer, 2013).

[18] K. Kadian, S. Garhwal, and A. Kumar, Quantum walk and its application domains: A systematic review, *Computer Science Review* **41**, 100419 (2021).

[19] S. Apers, S. Chakraborty, L. Novo, and J. Roland, Quadratic speedup for spatial search by continuous-time quantum walk, *Physical review letters* **129**, 160502 (2022).

[20] F. Magniez, M. Santha, and M. Szegedy, Quantum algorithms for the triangle problem, *SIAM Journal on Computing* **37**, 413 (2007).

[21] P. W. Jensen, C. Jin, P.-L. Dallaire-Demers, A. Aspuru-Guzik, and G. C. Solomon, Molecular realization of a quantum nand tree, *Quantum Science and Technology* **4**, 015013 (2019).

[22] Y. Wang, Z.-W. Cui, Y.-H. Lu, X.-M. Zhang, J. Gao, Y.-J. Chang, M.-H. Yung, and X.-M. Jin, Integrated quantum-walk structure and nand tree on a photonic chip, *Physical Review Letters* **125**, 160502 (2020).

[23] T. Kitagawa, M. S. Rudner, E. Berg, and E. Demler, Exploring topological phases with quantum walks, *Physical Review A* **82**, 033429 (2010).

[24] S. Dadras, A. Gresch, C. Groiseau, S. Wimberger, and G. S. Summy, Quantum walk in momentum space with a bose-einstein condensate, *Phys. Rev. Lett.* **121**, 070402 (2018).

[25] D. Xie, T.-S. Deng, T. Xiao, W. Gou, T. Chen, W. Yi, and B. Yan, Topological quantum walks in momentum space with a bose-einstein condensate, *Physical Review Letters* **124**, 050502 (2020).

[26] M. Kac, Random walk and the theory of brownian motion, *The American Mathematical Monthly* **54**, 369 (1947).

[27] A. Romanelli and et al., Decoherence in the quantum walk on the line, *Physica A: Statistical Mechanics and its Applications* **347**, 137 (2005).

[28] S. Chakrabarti and et al., Quantum algorithm for estimating volumes of convex bodies, *ACM Transactions on Quantum Computing* , 1 (2023).

[29] D. Wiater, T. Sowiński, and J. Zakrzewski, Two bosonic quantum walkers in one-dimensional optical lattices, *Phys. Rev. A* **96**, 043629 (2017).

[30] S. Anisur, K. Singh, and S. Choudhury, Directional quantum walks of two bosons on the hatano-nelson lattice, *arXiv preprint arXiv:2511.03613* (2025).

[31] S. Garnerone, P. Zanardi, and D. A. Lidar, Adiabatic quantum algorithm for search engine ranking, *Phys. Rev.*

Lett. **108**, 230506 (2012).

[32] P. Chawla, R. Mangal, and C. M. Chandrashekhar, Discrete-time quantum walk algorithm for ranking nodes on a network, *Quantum Information Processing* **19**, 1 (2020).

[33] D. A. Meyer, From quantum cellular automata to quantum lattice gases, *Journal of Statistical Physics* **85**, 551 (1996).

[34] D. A. Meyer, On the absence of homogeneous scalar unitary cellular automata, *Physics Letters A* **223**, 337 (1996).

[35] F. W. Strauch, Connecting the discrete-and continuous-time quantum walks, *Physical Review A* **74**, 030301 (2006).

[36] O. Mülken and A. Blumen, Continuous-time quantum walks: Models for coherent transport on complex networks, *Physics Reports* **502**, 37 (2011).

[37] N. B. Lovett, S. Cooper, M. Everett, M. Trevers, and V. Kendon, Universal quantum computation using the discrete-time quantum walk, *Physical Review A* **81**, 042330 (2010).

[38] A. M. Childs, On the relationship between continuous- and discrete-time quantum walk, *Communications in Mathematical Physics* **294**, 581 (2010).

[39] P. Kurzyński and A. Wójcik, Discrete-time quantum walk approach to state transfer, *Phys. Rev. A* **83**, 062315 (2011).

[40] S. R. Jackson, T. J. Khoo, and F. W. Strauch, Quantum walks on trees with disorder: Decay, diffusion, and localization, *Phys. Rev. A* **86**, 022335 (2012).

[41] R. Vieira, E. P. M. Amorim, and G. Rigolin, Entangling power of disordered quantum walks, *Phys. Rev. A* **89**, 042307 (2014).

[42] H. Lavicka, V. Potoček, T. Kiss, E. Lutz, and I. Jex, Quantum walk with jumps, *European Physical Journal D - EUR PHYS J D* **64** (2011).

[43] M. Pires, G. Di Molfetta, and S. Queirós, Multiple transitions between normal and hyperballistic diffusion in quantum walks with time-dependent jumps, *Scientific Reports* **9**, 19292 (2019).

[44] S. Das, S. Mal, A. Sen(De), and U. Sen, Inhibition of spreading in quantum random walks due to quenched poisson-distributed disorder, *Phys. Rev. A* **99**, 042329 (2019).

[45] S. Mukhopadhyay and P. Sen, Persistent quantum walks: Dynamic phases and diverging timescales, *Phys. Rev. Res.* **2**, 023002 (2020).

[46] M. A. Pires and S. M. D. Queirós, Quantum walks with sequential aperiodic jumps, *Phys. Rev. E* **102**, 012104 (2020).

[47] C. B. Naves, M. A. Pires, D. O. Soares-Pinto, and S. M. D. Queirós, Enhancing entanglement with the generalized elephant quantum walk from localized and delocalized states, *Phys. Rev. A* **106**, 042408 (2022).

[48] S. Salimi and R. Yosefjani, Asymptotic entanglement in 1d quantum walks with a time-dependent coined, *International Journal of Modern Physics B* **26**, 1250112 (2012).

[49] R. Vieira, E. P. Amorim, and G. Rigolin, Dynamically disordered quantum walk as a maximal entanglement generator, *Physical review letters* **111**, 180503 (2013).

[50] P. P. Rohde, G. K. Brennen, and A. Gilchrist, Quantum walks with memory provided by recycled coins and a memory of the coin-flip history, *Physical Review A* **87**, 052302 (2013).

[51] R. Vieira, E. P. Amorim, and G. Rigolin, Entangling power of disordered quantum walks, *Physical Review A* **89**, 042307 (2014).

[52] G. Di Molfetta and F. Debbasch, Discrete-time quantum walks in random artificial gauge fields, *Quantum Studies: Mathematics and Foundations* **3**, 293 (2016).

[53] M. Montero, Classical-like behavior in quantum walks with inhomogeneous, time-dependent coin operators, *Physical Review A* **93**, 062316 (2016).

[54] Q.-Q. Wang, X.-Y. Xu, W.-W. Pan, K. Sun, J.-S. Xu, G. Chen, Y.-J. Han, C.-F. Li, and G.-C. Guo, Dynamic-disorder-induced enhancement of entanglement in photonic quantum walks, *Optica* **5**, 1136 (2018).

[55] A. C. Orthey and E. P. Amorim, Weak disorder enhancing the production of entanglement in quantum walks, *Brazilian Journal of Physics* **49**, 595 (2019).

[56] S. Singh, R. Balu, R. Laflamme, and C. Chandrashekhar, Accelerated quantum walk, two-particle entanglement generation and localization, *Journal of Physics Communications* **3**, 055008 (2019).

[57] A. Buarque and W. d. S. Dias, Aperiodic space-inhomogeneous quantum walks: Localization properties, energy spectra, and enhancement of entanglement, *Physical Review E* **100**, 032106 (2019).

[58] M. A. Pires and S. M. Duarte Queirós, Negative correlations can play a positive role in disordered quantum walks, *Scientific Reports* **11**, 4527 (2021).

[59] P. Ghosh, K. Sen, and U. Sen, Response to glassy disorder in coin on spread of quantum walker, *arXiv: 2111.09827* (2022).

[60] C. B. Naves, M. A. Pires, D. O. Soares-Pinto, and S. M. D. Queirós, Quantum walks in two dimensions: controlling directional spreading with entangling coins and tunable disordered step operator, *Journal of Physics A: Mathematical and Theoretical* **56**, 125301 (2023).

[61] N. Linden and J. Sharam, Inhomogeneous quantum walks, *Physical Review A* **80**, 052327 (2009).

[62] A. P. Chatterjee and R. F. Loring, Effective medium approximation for random walks with non-markovian dynamical disorder, *Physical Review E* **50**, 2439 (1994).

[63] Y. Yin, D. Katsanos, and S. Evangelou, Quantum walks on a random environment, *Physical Review A* **77**, 022302 (2008).

[64] F. Nosrati, A. Laneve, M. K. Shadfar, A. Gerald, K. Mahdavipour, F. Pegoraro, P. Mataloni, and R. L. Franco, Readout of quantum information spreading using a disordered quantum walk, *JOSA B* **38**, 2570 (2021).

[65] C. Mendes, G. Almeida, M. Lyra, and F. de Moura, Localization properties of a discrete-time 1d quantum walk with generalized exponential correlated disorder, *Physics Letters A* **394**, 127196 (2021).

[66] A. Mandal, R. S. Sarkar, and B. Adhikari, Localization of two dimensional quantum walks defined by generalized grover coins, *Journal of Physics A: Mathematical and Theoretical* **56**, 025303 (2023).

[67] R. Duda, M. N. Ivaki, I. Sahlberg, K. Pöyhönen, and T. Ojanen, Quantum walks on random lattices: Diffusion, localization, and the absence of parametric quantum speedup, *Physical Review Research* **5**, 023150 (2023).

[68] C. Ampadu *et al.*, On some questions of c. ampadu associated with the quantum random walk, *Applied Mathematics* **5**, 3040 (2014).

- [69] T. Matsushita and H. F. Hofmann, Origin of meter fluctuations in weak measurement interactions, *Phys. Rev. A* **109**, 022224 (2024).
- [70] T. Yamasaki, H. Kobayashi, and H. Imai, Analysis of absorbing times of quantum walks, *Physical Review A* **68**, 012302 (2003).
- [71] E. Bach, S. Coppersmith, M. P. Goldschen, R. Joynt, and J. Watrous, One-dimensional quantum walks with absorbing boundaries, *Journal of Computer and System Sciences* **69**, 562 (2004).
- [72] L. C. Kwek and Setiawan, One-dimensional quantum walk with a moving boundary, *Phys. Rev. A* **84**, 032319 (2011).
- [73] P. Kuklinski and M. Kon, Absorption probabilities of quantum walks, *Quantum Information Processing* **17**, 1 (2018).
- [74] P. Kuklinski, Conditional probability distributions of finite absorbing quantum walks, *Phys. Rev. A* **101**, 032309 (2020).
- [75] S. Chandrasekhar, Stochastic problems in physics and astronomy, *Rev. Mod. Phys.* **15**, 1 (1943).
- [76] E. Bach, S. Coppersmith, M. P. Goldschen, R. Joynt, and J. Watrous, One-dimensional quantum walks with absorbing boundaries, *Journal of Computer and System Sciences* **69**, 562 (2004).
- [77] A. Mandal and U. Sen, Stronger resilience to disorder in 2d quantum walks than in 1d, *arXiv preprint arXiv:2312.16076* (2023).
- [78] G. B. Arfken and H. J. Weber, *Mathematical Methods for Physicists*, 3rd ed. (Academic Press, Orlando, FL, 1985) pp. 286–287.

Appendix A: Glassy Disorders in DTQWs

Before introducing the disorder in the walker's step length, the evolution of the quantum system was not considered random, and the randomness in the system was only in the results of measurement after a walk. Now, we introduce disorder in the evolution of the quantum system by making the length of the steps of the quantum walk random. In an ordered system, the walk evolves by taking the same step lengths at all the time steps. However, in a disordered system, the insertion of disorder is carried out in the walker's steps, such that after each time step, the walker moves following a step of any random length (l) related to the probability function $\text{pmf}(r; l)$ under consideration. In detail, a probability distribution of a variable outcome l is outlined as $\text{pmf}(r; l)$, where r denotes some suitable parameter of the given distribution. Now the walker can take a step of length l after each toss, unlike to the ordered situation, where the length of the step is taken to be 1 after each toss. From a mathematical perspective, when we include disorder, the shift operator, which has to be operated after the operation of the coin tossing operator, takes the form

$$\hat{S} = \sum_{n=-\infty}^{\infty} |n-l, L\rangle \langle n, L| + |n+l, R\rangle \langle n, R|, \quad (\text{A1})$$

unlike to Eq. (3). Here, l has to be chosen with specified probability $\text{pmf}(r; l)$ for some fixed parameters r .

In this paper, unless explicitly mentioned, we refer to the disorders employed in the system as *glassy disorders*. As an essential feature of the glassy disorder, the parameter r of the specified distribution $\text{pmf}(r; l)$ remains unchanged during a full walk. Below, we state the probability mass functions of the Poissonian, sub- and super-Poissonian distributions whose discrete outcomes serve the role of disorder.

Poisson distribution. In this distribution, the only parameter λ represents the mean value of the distribution and the mass function $\text{pmf}(\lambda; l)$ is defined as

$$\text{pmf}(\lambda, l) = \frac{\lambda^l e^{-\lambda}}{l!}.$$

Both the mean value and the variance of such a distribution are equal to λ .

Sub- and super-Poisson distributions. The probability distribution for which the variance is larger (smaller) than a Poisson distribution with the same mean value is called a super- (sub-) Poissonian distribution. For example, binomial and hypergeometric are sub-Poissonian distributions, whereas negative-binomial and geometric are super-Poissonian distributions.

Binomial distribution. The probability function for this distribution is

$$\text{pmf}(n, p; l) = \binom{n}{l} p^l (1-p)^{n-l},$$

where n and p are two free parameters of the distribution. The mean value and the variance of this distribution are np and $np(1-p)$, respectively. Clearly, $np > np(1-p)$, since $0 \leq p \leq 1$ is the probability value.

Hypergeometric distribution. The probability mass function of the hypergeometric distribution is

$$\text{pmf}(N, K, n; l) = \frac{\binom{K}{l} \binom{N-K}{n-l}}{\binom{N}{n}},$$

with N, K , and n as the free parameters. The mean value and the variance for the distribution are $\frac{nK}{N}$ and $\frac{nK(N-K)(N-n)}{N^2(N-1)}$, respectively.

Negative binomial distribution. The mass function of the specified distribution is

$$\text{pmf}(r, k; l) = \binom{l+r-1}{l} (1-k)^r k^l,$$

with r and k as parameters of the distribution. The mean and variance are $\frac{r(1-k)}{k}$, and $\frac{r(1-k)}{k^2}$, respectively.

Geometric distribution. The probability mass function of the geometric distribution is

$$\text{pmf}(k; l) = (1-k)^{l-1} k,$$

where k acts as a parameter. The mean and variance of this distribution can be derived as $\frac{1}{k}$ and $\frac{1-k}{k^2}$, respectively.

Appendix B

Here, we sketch the proof that the total absorption probability of a classical walker is 1 and does not depend on the distance of the absorber from the starting point of the walker.

Let us assume that the absorber is at the position $-m_1$ (without any loss of generality, we can assume that $m_1 \in \mathbb{Z}$ is positive). Let $P(-m_1)$ be the total probability of absorption of the walker starting from zero, and $p_t(-m_1)$ stands for the probability of absorption at $-m_1$ for the first time after t time steps. Clearly, $P(-1) = \frac{1}{2} + \frac{1}{2}P(-1)P(-1)$, which yields $P(-1) = 1$ [7]. Now to calculate $P(-2)$, which looks as

$$\frac{1}{2} \times \frac{1}{2} + \left(\frac{1}{2} \times \frac{1}{2} + \frac{1}{2} \times \frac{1}{2} \right) P(-2) + \frac{1}{2} \times \frac{1}{2} P(-2)P(-2),$$

which simplifies to $P(-2) = 1$.

Finally, consider $P(-m_1)$, which can be expressed as

$$P(-m_1) = \sum_{i=0}^{\infty} p_{m_1+2i}(-m_1). \quad (\text{B1})$$

Now, the following recurrence relations can be obtained for $m_1 > 2$, in a similar way as we calculated $P(-2)$.

$$\begin{aligned} p_{m_1}(-m_1) &= \frac{1}{4} p_{m_1-2}(-(m_1-2)), \\ p_{m_1+2}(-m_1) &= \frac{1}{4} p_{m_1}(-(m_1-2)) + \frac{1}{2} p_{m_1}(-m_1), \\ p_{m_1+4}(-m_1) &= \frac{1}{4} p_{m_1+2}(-(m_1-2)) + \frac{1}{2} p_{m_1+2}(-m_1) + \frac{1}{4} p_2(-2)p_{m_1}(m_1), \\ p_{m_1+6}(-m_1) &= \frac{1}{4} p_{m_1+4}(-(m_1-2)) + \frac{1}{2} p_{m_1+4}(-m_1) + \frac{1}{4} (p_4(-2)p_{m_1}(m_1) + p_2(-2)p_{m_1+2}(m_1)). \end{aligned}$$

Using Eq. (B1) and the above set of recurrence relations, we get

$$P(-m_1) = \frac{1}{4} P(-(m_1-2)) + \frac{1}{2} P(-m_1) + \frac{1}{4} P(-2)P(-m_1). \quad (\text{B2})$$

From Eq. (B2) and using $P(-2) = 1$, we get

$$P(-m_1) = P(-(m_1-2)). \quad (\text{B3})$$

Hence, $P(-1) = 1$, $P(-2) = 1$, and Eq. (B3) together imply that $P(-m_1) = 1$ for any $m_1 > 0$. Note that, following a similar approach presented above, we can show that $P(-m_1) = 1$ whenever m_1 is a negative integer.

Appendix C

In this section, we prove the divergence of the series given in Eq. (8) and the convergence of the series in Eq. (13). Before that, we briefly describe Raabe's Test for testing the convergence of a series of positive terms [78].

Raabe's Test: Consider an infinite series $\sum_n u_n$, where $u_n > 0$ for every n . Then, the series $\sum_n u_n$, converges if $E > 1$, diverges if $E < 1$, and no conclusion can be made if $E = 1$, where

$$E = \lim_{n \rightarrow \infty} n \left(\frac{u_n}{u_{n+1}} - 1 \right). \quad (\text{C1})$$

For convenience, we assume that m_1 is positive, then the series sum in Eq. (8) can be written in the following form since $t \geq m_1$.

$$\sum_{n=1}^{\infty} \frac{m_1(m_1 + 2n)!}{2^{m_1 + 2n} \left(\frac{m_1 + 2n + m_1}{2}\right)! \left(\frac{m_1 + 2n - m_1}{2}\right)!} = \frac{m_1}{2^{m_1}} \sum_{n=1}^{\infty} \frac{(m_1 + 2n)!}{4^n (m_1 + n)! n!}.$$

Now, let us calculate E as described in Eq. (C1) for the above expression.

$$\begin{aligned} E &= \lim_{n \rightarrow \infty} n \left(4 \frac{(m_1 + 2n)!}{(m_1 + 2n + 2)!} \frac{(n+1)!}{n!} \frac{(m_1 + n + 1)!}{(m_1 + n)!} - 1 \right) \\ &= \lim_{n \rightarrow \infty} n \left(\frac{(n+1)(n+1+m_1)}{(n+\frac{1+m_1}{2})(n+\frac{2+m_1}{2})} - 1 \right) \\ &= \lim_{n \rightarrow \infty} \frac{\frac{1}{2} + \frac{1+m_1}{n} - \frac{(1+m_1)(2+m_1)}{4n}}{1 + \frac{3+2m_1}{2n} + \frac{(1+m_1)(2+m_1)}{4n^2}} \\ &= \frac{1}{2} < 1. \end{aligned}$$

Hence, the series mentioned in Eq. (8) diverges by applying Raabe's test.

For the infinite series given in Eq. (13), we calculate E as follows.

$$E = \lim_{n \rightarrow \infty} n \left(\frac{4n-2}{4n+2} \left(\frac{(2n-2)!}{(2n)!} \right)^2 \left(\frac{n!(n+1)!}{(n-1)!n!} \right)^2 \left(\frac{2^{2n+1}}{2^{2n-1}} \right)^2 - 1 \right)$$

This can be simplified as

$$E = \lim_{n \rightarrow \infty} n \left(16 \left(\frac{4n-2}{4n+2} \right) \frac{n^2(n+1)^2}{(2n-1)^2(2n)^2} - 1 \right)$$

$$= \lim_{n \rightarrow \infty} n \left(\left(\frac{n - \frac{1}{2}}{n + \frac{1}{2}} \right) \frac{(n+1)^2}{(n - \frac{1}{2})^2} - 1 \right)$$

$$E = \lim_{n \rightarrow \infty} n \left(\frac{(n+1)^2}{n^2 - \frac{1}{4}} - 1 \right)$$

$$= \lim_{n \rightarrow \infty} n \left(\frac{2n + \frac{5}{4}}{n^2 - \frac{1}{4}} \right) = \lim_{n \rightarrow \infty} \left(\frac{2 + \frac{5}{4n}}{1 - \frac{1}{4n^2}} \right) = 2 > 1$$

Thus, by Raabe's test, the series sum in Eq. (13) converges.